International Journal of Control, Energy and Electrical Engineering (CEEE)
Vol.9 pp.20-25

Optical absorption of new n-doped GaN0.38yAs1-1.38ySby/GaAs QWs suitable for the design of 0.8 - 1 eV solar cells

C.Bilel[#1], A. Rebey[*]

[#] *Physics Department, College of Science, Jouf University, P.O. Box: 2014, Sakaka, Saudi Arabia*
[1]chakroun@ju.edu.sa

[*] *Qassim University, College of Science, Kingdom of Saudi Arabie*

***Abstract*— We investigated the optical absorption of n-doped GaN0.38yAs1-1.38ySby/GaAs quantum wells (QWs) using a self-consistent calculation combined with the 16-band anti-crossing model. GaNAsSb material seems to be a potential alternative for GaAs-based photodetectors operating at 0.8 - 1 eV energy range. The increase of the well width from 4 to 10 nm in GaN0.38yAs1-1.38ySby/GaAs QWs caused a red-shift of the fundamental transition energy accompanied with a significant decrease of the absorption coefficient. The wavelength emission of the studied QWs achieved the values 0.8 and 0.95 eV for specific values of Sb composition. A rise of doping density induced an increase of . The Stark effect on energy and was also discussed. Additionally, was adjusted in order to obtain the energies 0.8 and 0.95 eV of the electrically polarized GaNAsSb/GaAs QWs.**

***Keywords*— GaNAsSb/GaAs QWs; Absorption coefficient; n doping; Stark effect; energy range 0.8 – 1 eV.**

I. Introduction

Over the past few years, GaNAsSb material has considered to be an alternative candidate for GaAs-based 0.8 - 1 eV photodetectors [1,2] and photovoltaic cells [3,4]. These materials show a rapid band gap reduction covering a large infrared range [5,6]. The dependence of the band gap energy of GaN_xAs_{1-x} alloys on the N composition can be theoretically exhibited by using the conduction band anticrossing model (C-BAC). The rate of band gap reduction for this material was found to be around 180 meV/%N [7-9]. For $GaSb_yAs_{1-y}$, the Sb composition dependence of the band gap energy can be described by the valence band anticrossing model (V-BAC). This alloy displays 16 meV/%Sb as a rate of the band gap reduction [10,11]. The combination of V-BAC and C-BAC models offers the possibility of examining the electronic band structure of $GaN_xAs_{1-x-y}Sb_y$ quaternary alloy [12,13]. The *x* and *y*-dependence of the band gap energy of $GaN_xAs_{1-x-y}Sb_y$ can be modeled in a large composition range ($0 < x < 0.06$ and $0 < y < 0.30$) [14]. The simultaneous incorporation of N and Sb atoms affects the conduction and valence bands leading to a rapid reduction of band gap energy which reached a minimum value of 0.5 eV (*i.e.* 2.48 µm). Experimentally, the optical measurements of the elaborated $GaN_xAs_{1-x-y}Sb_y$/GaAs structures show that the value of band gap energy is around 0.80 eV (*i.e.* 1.55 µm) for the couples ($x_N = 0.03$, $y_{Sb} = 0.15$) [15], ($x_N = 0.03$, $y_{Sb} = 0.20$) [16] and ($x_N = 0.01$, $y_{Sb} = 0.31$) [17]. The energy 0.95 eV was obtained for the couples ($x_N = 0.02$, $y_{Sb} = 0.12$) [5] and ($x_N = 0.02$, $y_{Sb} = 0.13$) [18]. Moreover, the subbands and inter-band transition of un-doped GaAs/$GaN_xAs_{1-x-y}Sb_y$/GaAs QWs were calculated using the envelope function approximation [19]. The study of *n* doping and Stark effects on the band structure and inter-band transition of GaAs/$GaN_xAs_{1-x-y}Sb_y$/GaAs single quantum well (SQW) can be useful to enhance the optical absorption process at the energies 0.8 and 0.95 eV.

The aim of this work is to investigate the *n* doping effect on the electronic band structure and optical absorption of GaAs/$GaN_xAs_{1-x-y}Sb_y$/GaAs SQW. The increase of the well width from 4 to 10 nm causes a red-shift of the fundamental transition energy as well as a decrease of the absorption coefficient. Specific values of Sb composition give rise to the energies emissions 0.8 and 0.95 eV of un-doped SQW. Owing to doping effect, the absorption process is enhanced. The Stark effect on the optical transition and absorption was also examined. Sb composition was adjusted in order to obtain electrically polarized GaAs/$GaN_xAs_{1-x-y}Sb_y$/GaAs SQW operating exactly at 0.8 and 0.95eV.

The (16×16) Hamiltonian can describe the electronic band structure of bulk GaNxAs1-x-ySby [20,21]:

$$H_{16\times16} = \begin{pmatrix} H_{8\times8}^{mod} & & V_{N(2\times8)} \\ & & V_{Sb(6\times8)} \\ V_{N(8\times2)} & V_{Sb(8\times6)} & H_{N,Sb(8\times8)} \end{pmatrix} \quad \textbf{(1a)}$$

where $H_{8\times8}^{mod}$ is the modified (8×8) k.p matrix by adding ΔECBM, ΔEVBM and ΔEso (bands edges offsets between GaAs and GaSb) to the diagonal elements [21]. $H_{N,Sb(8\times8)}$) matrix is formed by the energies levels of N atoms (EN) and Sb atoms (ESb and spin-orbit splitting level ESb-so):

ISSN 2356-5608

$$H_{N,Sb(8\times8)} = \begin{pmatrix} E_N & 0 & 0 & 0 & 0 & 0 & 0 & 0 \\ 0 & E_N & 0 & 0 & 0 & 0 & 0 & 0 \\ 0 & 0 & E_{Sb} & 0 & 0 & 0 & 0 & 0 \\ 0 & 0 & 0 & E_{Sb} & 0 & 0 & 0 & 0 \\ 0 & 0 & 0 & 0 & E_{Sb} & 0 & 0 & 0 \\ 0 & 0 & 0 & 0 & 0 & E_{Sb} & 0 & 0 \\ 0 & 0 & 0 & 0 & 0 & 0 & E_{Sb-so} & 0 \\ 0 & 0 & 0 & 0 & 0 & 0 & 0 & E_{Sb-so} \end{pmatrix} \quad \textbf{(1b)}$$

$V_{Sb(6\times8)}$ matrix is formed by the term $\mathrm{V}_{Sb}(\mathrm{y}) = C_{Sb}\, y^{1/2}$ describing the coupling between Sb isoelectronic localized states and extended valence band (VB):

$$V_{Sb(6\times8)} = \begin{pmatrix} 0 & 0 & \mathrm{V}_{Sb}(\mathrm{y}) & 0 & 0 & 0 & 0 & 0 \\ 0 & 0 & 0 & \mathrm{V}_{Sb}(\mathrm{y}) & 0 & 0 & 0 & 0 \\ 0 & 0 & 0 & 0 & \mathrm{V}_{Sb}(\mathrm{y}) & 0 & 0 & 0 \\ 0 & 0 & 0 & 0 & 0 & \mathrm{V}_{Sb}(\mathrm{y}) & 0 & 0 \\ 0 & 0 & 0 & 0 & 0 & 0 & \mathrm{V}_{Sb}(\mathrm{y}) & 0 \\ 0 & 0 & 0 & 0 & 0 & 0 & 0 & \mathrm{V}_{Sb}(\mathrm{y}) \end{pmatrix} \quad \textbf{(1c)}$$

CSb is a fitting parameter taken equal to 1.05 eV [10]. Similar to Sb levels interactions with VB states, the matrix $V_{N(2\times8)}$ is composed of the term $\mathrm{V}_N(\mathrm{x}) = C_N\, x^{1/2}$ and reveals the coupling between the N localized states and the extended conduction band (CB) states. The matrix $V_{N(2\times8)}$ can be written as:

$$V_{N(2\times8)} = \begin{pmatrix} \mathrm{V}_N(\mathrm{x}) & 0 & 0 & 0 & 0 & 0 & 0 & 0 \\ 0 & \mathrm{V}_N(\mathrm{x}) & 0 & 0 & 0 & 0 & 0 & 0 \end{pmatrix} \quad \textbf{(1d)}$$

CN is a fitting parameter equal to 2.7 eV [22]. The BAC parameters used in this work are reported in TABLE I. GaNxAs1-x-ySby material can be lattice-matched to GaAs with a concentration ratio $x/y = 0.38$ [22].

TABLE I

A Summary of BAC parameters used in this work. EN represents the N localized level. ESb and ESb-so are Sb localized levels. CN and CSb are fitting parameters. ΔE_{CBM}, ΔE_{VBM} and ΔE_{SO} are conduction, valence and spin-orbit splitting band edges offsets, respectively.

Parameters	EN (eV)	CN (eV)	ESb (eV)	ESb-so (eV)
GaNAsSb	1.65 [10,20]	2.7 [10,20]	-1.0 [10]	-1.6 [10]

Parameters	CSb (eV)	ΔE_{VBM} (eV)	ΔE_{CBM} (eV)	ΔE_{SO} (eV)
GaNAsSb	1.05 [10]	0.5 [10]	-0.1 [10]	0.09 [10]

For GaNxAs1-x-ySby/GaAs QWs, subbands and confined potential can be computed using the envelope function approximation [23,24]. The total Hamiltonian is given by the following expression: $H = H_{\parallel} + H_z$, where $H_{\parallel} = -\frac{\hbar^2}{2m^*_{\parallel i}}\nabla^2_{\parallel}$ is the Hamiltonian of system in a direction parallel to the GaNAsSb-GaAs interface. $m^*_{\parallel i}$ ($i = e$ for electron and h for heavy hole) is the carrier effective mass in $\boldsymbol{k}_{\parallel}$ -direction. $H_z = -\frac{\hbar^2}{2}\nabla_z \frac{1}{m^*_{ij}(z)}\nabla_z + V(z)$ is the Hamiltonian of the system in quantizing z-direction where $V(z)$ is the total potential energy. For un-doped GaNAsSb/GaAs QWs, $V(z)$ is restricted to the band discontinuity $U_B(z)$ between the GaAs barrier and GaNAsSb well. For n doped GaNAsSb/GaAs QWs, the coupled Schrödinger-Poisson equations are written as [25,26]:

$$\left(-\frac{\hbar^2}{2}\nabla_z \frac{1}{m^*_{ij}(z)}\nabla_z + U_B(z) + U_H(z) + U_{xc}(z) + eFz\right)\varphi_j(z) = E_j\,\varphi_j(z) \quad \textbf{(2a)}$$

$$\frac{d^2 U_H(z)}{dz^2} = \frac{e^2}{\varepsilon_0\varepsilon_r}(N_d(z) - n(z)) \quad \textbf{(2b)}$$

E_j and $\varphi_j(z)$ are, respectively, the eigenvalues and eigenvectors of H_z. The envelope wavefunctions $\varphi_j(z)$ satisfy the boundary condition at the interfaces $(z = 0)$ and $(z = L_w)$. $U_H(z)$ and $U_{xc}(z)$ are the Hartree and exchange-correlation potentials respectively. $U_H(z)$ is obtained by solving the Poisson equation discretized using the finite differences method (FDM) taking into account the boundary conditions. The exchange-correlation potential $U_{xc}(z)$ is induced by the many-body effects [27]. eFz is the potential induced by the applied electric field. $N_d(z)$ and $n(z)$ are the donor and confined electron density respectively. e is the absolute value of the electron charge and $\varepsilon_0\varepsilon_r$ is the local dielectric constant of the medium. The equations (2a) and (2b) were discretized along the confinement z-direction using the FDM.

ISSN 2356-5608

To solve the coupled Schrödinger-Poisson equations, an iterative procedure was used. More calculation details of subbands, confined electron density, Fermi level, absorption coefficient and quantum confinement Stark effect are reported in references [26,28].

II. RESULTS AND DISCUSSION

We have theoretically examined the electronic band structure of un-doped GaN*x*As*1-x-y*Sb*y*/GaAs SQW. In fact, quantum well GaN*x*As*1-x-y*Sb*y* layer is lattice-matched to barrier GaAs using the ratio $x/y = 0.38$ [22]. Sb introduces two localized levels E_{Sb} and E_{Sb-so} situated at 1.0 and 1.6 eV below the GaAs VB edge, respectively [10]. N localized level E_N is positioned at 0.23 eV above the GaAs CB edge [22]. According to the QWs confinement conditions, the well width L_w domain was optimized basing on the following expressions:

$$L_w^{min} = \pi\hbar/\sqrt{2m_e^w U_B} \quad \textbf{(3a)}$$

$$L_w^{max} = \frac{\lambda_{th}}{\pi}\cos^{-1}\sqrt{E_{th}/\left(U_B\frac{m_e^w}{m_e^b} + E_{th}\left(1-\frac{m_e^w}{m_e^b}\right)\right)} \quad \textbf{(3b)}$$

where m_e^w and m_e^b are the electron effective mass of well GaNAsSb and barrier GaAs, respectively. $\lambda_{th} = 2\pi\hbar/\sqrt{2m_e^w k_B T}$ and $E_{th} = k_B T$ are the De Broglie thermal wavelength and the thermal energy, respectively. For GaNAsSb/GaAs QWs QW, L_w^{min} and L_w^{max} are equal to 3.6 and 11.3 nm, respectively. As shown in the inset of Fig. 1, the fundamental inter-band transition T_{e1-h1} is between the electron subband *e1* and the heavy hole subband *h1*. Fig. 1 shows the dependence of the transition energy T_{e1-h1} on the Sb composition y_{Sb} (*i.e.* N composition $x_N = 0.38\ y_{Sb}$) for L_w varying from 4 to 10 nm. The increase of y_{Sb} induces a significant decrease of T_{e1-h1}. Due to the band anticrossing effect, the coupling interaction between Sb localized levels and the valence band maximum VBM of GaAs leads to a rise of the VBM of GaAs*1-y*Sb*y* [12-14]. The coupling interaction between N level and the conduction band minimum CBM of GaAs makes the CBM of GaN$_x$As$_{1-x}$ move downward [7-9]. Along the z-quantizing direction of the studied GaAs/GaN*0.38y*As*1-1.38y*Sb*y*/GaAs SQW, the confined electrons level e1 and heavy holes level h1 move downward and upward with the rise of Sb composition, respectively. The wavelength of the fundamental transition λ_{Te1-h1} achieves 1.3 and 1.55 µm (*i.e.* 0.95 and 0.80 eV, respectively) for specific values of y_{Sb} (as displayed in Fig. 1).

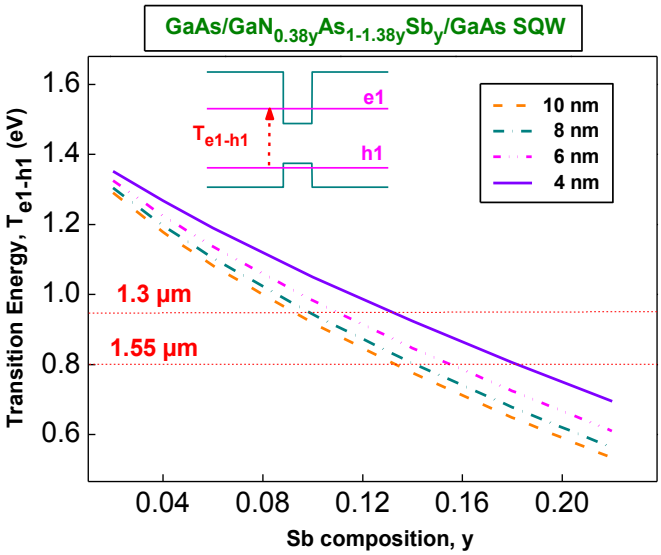

a.

Fig. 1. Dependence of the transition energy T_{e1-h1} of GaAs/GaN$_{0.38y}$As$_{1-1.38y}$Sb$_y$/GaAs SQW on Sb composition y_{Sb} for different values of the well width L_w. The band diagram of subbands is presented in Inset figure.

The variation of the absorption coefficient α_{abs} of GaAs/GaN*0.38y*As*1-1.38 y*Sb*y*/GaAs SQW as a function of the well width L_w is shown in Fig. (2a and 2b). For $L_w = 4\ nm$, λ_{Te1-h1} can be equal to 1.3 µm and 1.55 µm for $y_{Sb} = 13.0\ \%$ and $18.1\ \%$, respectively. The absorption coefficient magnitude $\alpha_{abs}^{T_{e1-h1}}$ is around $5.8\ 10^4$ and $6.9\ 10^4\ cm^{-1}$, respectively. Then, the increase of L_w from 4 to 10 nm induces a significant red-shift of T_{e1-h1} energy. To correct this shift, we adjusted the y_{Sb} for each used value of L_w. The adjusted y_{Sb} is equal to 10.8 %, 9.7 % and 9.1 % for $L_w = 6\ nm$, 8 nm and 10 nm, respectively. Likewise, the rise of L_w causes a decrease of $\alpha_{abs}^{T_{e1-h1}}$. For $\lambda_{Te1-h1} = 1.3\ \mu m$, $\alpha_{abs}^{T_{e1-h1}}$ reduces to $9.7\ 10^3\ cm^{-1}$ when L_w reaches 10 nm. For $\lambda_{Te1-h1} = 1.55\ \mu m$, $\alpha_{abs}^{T_{e1-h1}}$ decreases to $9.9\ 10^3\ cm^{-1}$ for $L_w = 10\ nm$. We noted the presence of two allowed transition T_{e1-h3} and T_{e1-h2} in the absorption spectra for $L_w \geq 8\ nm$, as shown in the insets zoom figures. Experimentally, Ohtani et al. [29] investigated the well width dependence of optical absorption in *n*-doped InAs/AlSb quantum structures. They signaled a red-shift of the absorption peak with increasing the well width.

ISSN 2356-5608

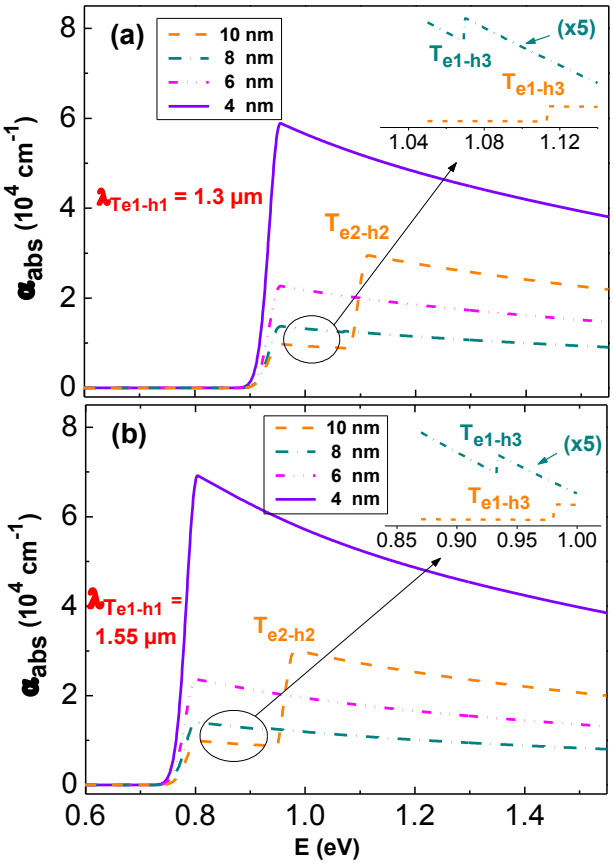

Fig. 2. Well width dependence of the absorption coefficient α_{abs} of GaAs/GaN$_{0.38y}$As$_{1-1.38y}$Sb$_y$/GaAs SQW for T_{e1-h1} equal to (a) 1.3 µm and (b) 1.55 µm.

In order to enhance the optical absorption process, we have studied the *n* doping effect on the electronic and optical properties of GaAs/GaN*0.38y*As*1-1.38 y*Sb*y*/GaAs SQW. The dependence of the fundamental transition T_{e1-h1} energy on the in-plane donor density N_d^{2D} is presented in Fig. 3a. The well width is $L_w = 4\ nm$. The Sb compositions give rise to $\lambda_{Te1-h1} = 1.3$ and 1.55 µm are 13.0 % and 18.1 %, respectively. The used N_d^{2D} range is between $1\ 10^{11}$ and $3\ 10^{12}\ cm^{-2}$. Owing to *n* doping effect, we have found that T_{e1-h1} energy shifts of 10 meV to higher energies. The obtained behavior is mainly due to the band-bending effect at the interface GaNAsSb (well) –GaAs (barrier). The rise of doping density causes the change of subbands positions and the enhancement of the electrons confinement. Likewise, we signaled in our previous work [25] a blue-shift (~10 meV) in *n*-doped GaAs/GaN*0.58y*As*1-1.58y*Bi*y*/GaAs QWs when the in-plane doping density reaches $2.2\ 10^{12}\ cm^{-2}$. In another study, Kim et al. [30] studied the doping effect on the optical properties of $GaAs_{.76}Sb_{.24}/In_{.26}Ga_{.74}N_{.06}As_{.94}$/GaAs QWs. They stated that the fundamental transition shifts of 20 meV to blue when the in-plane carrier density increases to 5 10^{12} cm^{-2}. It should be noted that the difference of the transition energy shift value of GaN*0.38y*As*1-1.38 y*Sb*y*/GaAs QWs compared to other systems may be due to the difference in their physical properties such as the total confining potential, range of doping density and carrier effective masses. On the other hand, we suggested adjusting the Sb composition y_{Sb} for each value of N_d^{2D} in order to keep the fundamental transition wavelength $\lambda_{T_{e1-h1}}$ equal to 1.3 and 1.55 µm.

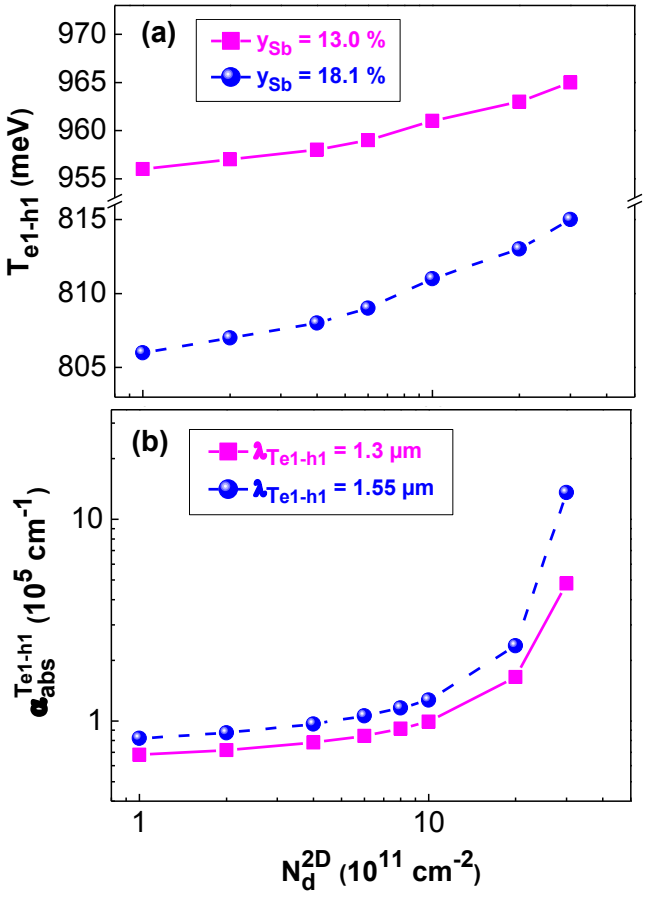

Fig. 3. Variation of (a) the transition energy T_{e1-h1} and (b) the absorption coefficient magnitude $\alpha_{abs}^{T_{e1-h1}}$ of GaAs/GaN$_{0.38y}$As$_{1-1.38y}$Sb$_y$/GaAs SQW as a function of the in-plane donor density N_d^{2D}.

In Fig. 3b, we plotted the variation of the absorption coefficient magnitude $\alpha_{abs}^{T_{e1-h1}}$ at the fundamental transition $T_{e1-h1} = 1.3$ and 1.55 µm as a function of the in-plane donor density N_d^{2D}. In fact, y_{Sb} values are in the ranges 13.1 – 13.4 % and 18.3 – 18.6 % for $\lambda_{T_{e1-h1}} = 1.3\ \mu m$ and $1.55\ \mu m$, respectively. For $\lambda_{T_{e1-h1}} = 1.3\ \mu m$, we found

ISSN 2356-5608

that $\alpha_{abs}^{T_{e1-h1}}$ increases from $6.8\ 10^4$ to $4.8\ 10^5\ cm^{-1}$ with increasing N_d^{2D} from $1\ 10^{11}$ to $3\ 10^{12}\ cm^{-2}$. In the same donor density range and for $\lambda_{T_{e1-h1}} = 1.55\ \mu m$, $\alpha_{abs}^{T_{e1-h1}}$ rises from $8.2\ 10^4$ to $13.6\ 10^5\ cm^{-1}$. This behavior was reported in the study of InGaN/GaN LEDs structures [31] and *n*-doped GaNAsBi/GaAs QWs and [25].On the other hand, Tan et al. [32] experimentally investigated the absorption in GaNAsSb/GaAs *p-i-n* photodetectors at the wavelength 1.3 µm. They stated that the absorption coefficient is about 1.3 10^4 cm^{-1}.

We have investigated the effect of the applied electric field on the optical absorption and inter-band transition in n-doped GaAs/GaN0.38yAs1-1.38 ySby/GaAs SQW. The in-plane donor density N_d^{2D} is equal to $3\ 10^{12}\ cm^{-2}$. Fig. 4a exhibits that without an applied electric field $F = 0\ kV/cm$, the use of Sb compositions 13.4 % and 18.6 % gives rise to a fundamental transition T_{e1-h1} equal to 0.95 (i.e. 1.3 µm) and 0.80 eV (i.e. 1.55 µm), respectively. Under an external electric field of up to $F = 140\ kV/cm$, the fundamental transition T_{e1-h1} energy shifts (~20 meV) to lower energies due to the quantum confined Stark effect. This red shift can be attributed to the modification of the electron and hole subbands under the effect of the applied electric field [33]. The Stark effect is more pronounced for holes as a consequence of their heavier effective masses and the lower valence band edge offset [34]. In order to maintain the wavelength $\lambda_{T_{e1-h1}}$ at 1.3 µm and 1.55 µm for each used value of the applied electric field, we adjusted the Sb composition y_{Sb} as shown in Fig. 4b. The dependence of the absorption coefficient magnitude $\alpha_{abs}^{T_{e1-h1}}$ at the fundamental transition T_{e1-h1} on the electric field F is displayed in Fig. 4c. For $\lambda_{T_{e1-h1}} = 1.3\ \mu m$, $\alpha_{abs}^{T_{e1-h1}}$ decreases from $4.8\ 10^5\ cm^{-1}$ to $4.2\ 10^4\ cm^{-1}$ when F increases from zero up to 140 kV/cm. For $\lambda_{T_{e1-h1}} = 1.55\ \mu m$, $\alpha_{abs}^{T_{e1-h1}}$ decreases from $13.6\ 10^5\ cm^{-1}$ to $4.7\ 10^4\ cm^{-1}$ with increasing F to the value of 140 kV/cm. In another study, Kuo et al. [35] investigated the Stark effect the on absorption coefficient spectra of Ge/SiGe QWs operating at 1.55 µm. They signaled that the absorption coefficient magnitude decreases from 104 cm-1 to 2 103 cm-1 when the bias voltage rises from zero to 2 V. The theoretical optimization of the Stark effect on the optoelectronic properties of such QWs improves the absorption process at the telecomm wavelengths 1.3 and 1.55 µm. The present investigation could be useful for the elaboration of highly efficient photodetectors based on n-doped GaNAsSb/GaAs QWs.

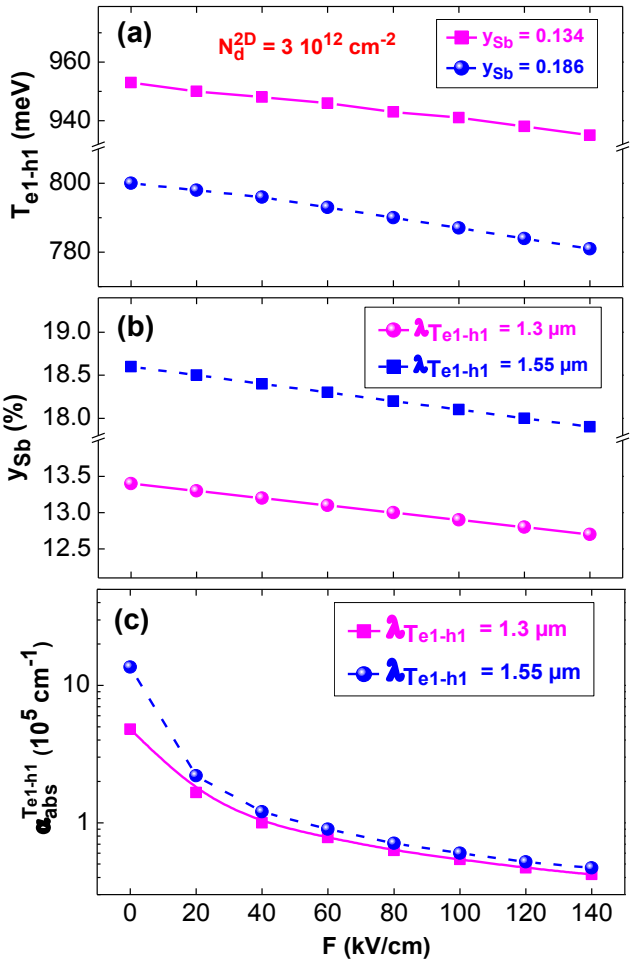

Fig. 4. Electric field dependence of (a) the transition energy T_{e1-h1}, (b) the adjusted value of Sb composition y_{Sb} and (c) the absorption coefficient magnitude $\alpha_{abs}^{T_{e1-h1}}$ of GaAs/$GaN_{0.38y}As_{1-1.38y}Sb_y$/GaAs SQW.

III. CONCLUSION

In summary, we have theoretically investigated the n doping effect on the electronic and optical absorption of lattice-matched GaAs/GaN0.38yAs1-1.38 ySby/GaAs SQW operating at 1.3 and 1.55 µm. We have performed a self-consistent calculation combined with (16×16) BAC model. For each value well width ranging from 4 to 10 nm, the use of specific Sb composition gives rise to the wavelengths emissions and . The increase of causes a significant decrease of absorption coefficient magnitude . This latter is enhanced to when the studied SQW is n doped with of up to . The Stark shift (∟20 meV) of the fundamental transition energy is stated when SQW is under an applied electric field F of up to 140 kV/cm. Sb composition is adjusted for each value of F to keep at 1.3 and 1.55 µm. The increase of the external electric field induces a slight decrease of the absorption coefficient.

ISSN 2356-5608

ACKNOWLEDGMENT

We gratefully acknowledge the financial support from the "Direction Générale de la Recherche Scientifique et de la Technologie" (DGRST), Tunisia.

REFERENCES

[1] S. Fedderwitz, A. Stöhr, S. F. Yoon, K. H. Tan, M. Weiß, W. K. Loke, A. Poloczek, S. Wicaksono, D. Jäger, Appl. Phys. Lett. 93 (2008) 033509.
[2] H. Luo, J.A. Gupta, H.C. Liu, Appl. Phys. Lett. 96 (2005) 211121.
[3] K.H. Tan, W.K. Loke, S. Wicaksono, D. Li, Y.R. Leong, S.F. Yoon, P. Sharma, T. Milakovich, M.T. Bulsara, E. A. Fitzgerald, Appl. Phys. Lett. 104 (2014) 103906.
[4] A. Marcos, N. Faleev, R.R. King, C.B. Honsberg, J. Vac. Technol. B 34 (2016) 02L106-1.
[5] Y.T. Lin, T.C. Ma, T.Y. Chen, H.H. Lin, Appl. Phys. Lett. 93 (2008) 171914.
[6] S.A. Lourence, M.A.T. da Silva, I.F.L. Dias, J.L.Duarte, J.C. Harmand, J.Phys.:Condens. Matter. 23 (2011) 325801.
[7] K. Uesugi, N. Morooka, I. Suemune, Appl. Phys. Lett. 74 (1999) 1254
[8] J. Wu, W. Shan, W. Walukiewicz, Semicond. Sci. Technol. 17 (2002) 860
[9] W. Shan, W. Walukiewicz, K.M. Yu, J.W. Ager III, E.E. Haller, J.F. Geisz, D.J. Friedman, J.M. Olson, S.R. Kurtz, H.P. Xin, C.W. Tu, Phys. Status Solidi B 223 (2001) 75.
[10] K. Alberi, J. Wu, W. Walukiewicz, K.M. Yu, O.D. Dubon, S.P. Watkins, C.X. Wang, X.
[11] Liu, Y.-J. Cho, J. Furdyna, Phys. Rev. B 75 (2007) 045203.
[12] R. Teissier, D. Sicault, J.C. Harmand, G. Ungaro, G. Le Roux, L. Largeau, J. Appl. Phys. 89 (2001) 5473.
[13] K.I. Lin, K.L. Lin, B.W. Wang, H.H. Lin, J.S. Hwang, Appl. Phys. Express 6 (2013) 121202.
[14] N. Ben Sedrine, C. Bouhafs, J.C. Harmand, R. Chtourou, V. Darakchieva, Appl. Phys. Lett. 97 (2010) 201903.
[15] C.Z. Zhao, H.F. Guo, T. Wei, S.S. Wang, K.Q. Lu, Physica B: Phys. Cond. Matter. 485 (2016) 35.
[16] J.C. Harmand, G. Ungaro, J. Ramos, E.V.K. Rao, G. Saint-Girons, R. Teissier, G. Le Roux, L. Largeau, G. Patriarche, J. Cryst. Growth 227 (2001) 553.
[17] J.C. Harmand, A. Caliman, E.V.K. Rao, L. Largeau, J. Ramos, R. Teissier, L. Travers, G. Ungaro, B. Theys, I.F.L. Dias, Semicond. Sci. Technol. 17 (2002) 778.
[18] M. Gladysiewicz, R. Kudrawiec, M.S. Wartak, IEEE J. Quant. Electron. 50 (2014) 996.
[19] S.A. Lourenço, I.F.L. Dias, L.C. Poças, J.L. Duarte, J.B.B. de Oliveira, J.C. Harmand, J. Appl. Phys. 93 (2003) 4475.
[20] F. Bousbih, S. Ben Bouzid, R. Chtourou, F.F. Charfi, J.C. Harmand, G. Ungaro, Mater. Sci. Eng. C 21 (2002) 251.
[21] M.M. Habchi, A. Ben Nasr, A. Rebey, B. El Jani, Infrared Phys. Technol. 61 (2013) 88.
[22] D.P. Samajdar, U. Das, A.S. Sharma, S. Das, S. Dhar, Curr. Appl. Phys. 16 (2016) 1687.
[23] I. Vurgaftman, J.R. Meyer, J. Appl. Phys. 94 (2003) 3675.
[24] G. Bastard, Wave Mechanics Applied to Semiconductor Heterostructures, Les Editions de Physique, Les Ulis Cedex, France, 1990.
[25] A. Ben Nasr, M.M. Habchi, C. Bilel, A. Rebey, B. El Jani, Journal of Semiconductors 49 (2015) 593.
[26] C. Bilel, M.M. Habchi, A. Rebey, B. El Jani, Physica E Low Dimens. Syst. Nanostruct. 69 (2015) 232.
[27] C. Bilel, M.M. Habchi, A. Rebey, B. El Jani, Thin Solid Films 581 (2015) 70.
[28] A. Ben Jazia, H. Merjri, H. Maaref, K. Souissi, Semicond. Sci. Technol. 12 (1997) 1388 and references therein.
[29] M.M. Habchi, C. Bilel, A. Ben Nasr, A. Rebey, B. El Jani, Mater. Sci. Semicond. Process. 28 (2014) 108.
[30] K. Ohtani, N. Matsumoto, H. Sakuma, H. Ohno, Appl. Phys. Lett. 82 (2003) 37.
[31] H.Y. Ryu, K.S. Jeon, M.G. Kang, Y. Choi, J.S. Lee, Opt. Express. 21 (2013) A190.
[32] K.H. Tan, S.F. Yoon, W.K. Loke, S. Wicaksono, T.K. Ng, K.L. Lew, A. Stöhr, S. Fedderwitz, M. Weiβ, D. Jäger, N. Saadsaoud, E. Dogheche, D. Decoster, J. Chazelas, Opt. Express. 16 (2008) 7720.
[33] A. Dimoulas, K.P. Giapis, J. Leng , G. Halkias, K. Zekentes, A. Christouc, J. Appl. Phys. 72 (1992) 1912.
[34] L. Vina, R.T. Collins, E.E. Mendez, W.I. Wang, L.L. Chang, L. Esaki, Superlattices and Microstructures 3 (1987) 9.
[35] Y. Kuo, Y. K. Lee, Y. Ge, S. Ren, J. E. Roth, T. I. Kamins, D. A. B. Miller, J. S. Harris, IEEE J. Sel. Topics Quantum Electron. 11 (2005) 338.

ISSN 2356-5608